ChemPubSoc Europe

DOI: 10.1002/celc.201500505

CHEMELECTROCHEM Articles

A Re-evaluation of Electron-Transfer Mechanisms in Microbial Electrochemistry: *Shewanella* Releases Iron that Mediates Extracellular Electron Transfer

Joseph Oram and Lars J. C. Jeuken*[a]

Exoelectrogenic bacteria can couple their metabolism to extracellular electron acceptors, including macroscopic electrodes, and this has applications in energy production, bioremediation and biosensing. Optimisation of these technologies relies on a detailed molecular understanding of extracellular electron-transfer (EET) mechanisms, and *Shewanella oneidensis* MR-1 (MR-1) has become a model organism for such fundamental studies. Here, cyclic voltammetry was used to determine the relationship between the surface chemistry of electrodes (modified gold, ITO and carbon electrodes) and the EET mechanism. On ultra-smooth gold electrodes modified with self-assembled monolayers containing carboxylic-acid-terminated thiols, an EET pathway dominates with an oxidative catalytic onset at 0.1 V versus SHE. Addition of iron(II)chloride enhances the catalytic current, whereas the siderophore deferoxamine abolishes this signal, leading us to conclude that this pathway proceeds via an iron mediated electron transfer mechanism. The same EET pathway is observed at other electrodes, but the onset potential is dependent on the electrolyte composition and electrode surface chemistry. EET pathways with onset potentials above −0.1 V versus SHE have previously been ascribed to direct electron-transfer (DET) mechanisms through the surface exposed decaheme cytochromes (MtrC/OmcA) of MR-1. In light of the results reported here, we propose that the previously identified DET mechanism of MR-1 needs to be re-evaluated.

1. Introduction

Microbial electrochemical systems (MESs) interface exoelectrogenic microbes to electrodes and exploit them for useful applications, such as biosensing, bioremediation, chemical synthesis and energy production.[1,2] Unfortunately, the performance of MESs, especially for energy production, is relatively low.[1] The general approach to increase the performance of MESs is to engineer the microbe and/or the electrode surface to increase electron transfer (ET) efficiency. This requires a detailed fundamental understanding of extracellular electron transfer (EET), and species from the *Geobacter* and *Shewanella* genus have been studied extensively for this purpose.[3,4] *Geobacter* sp. generally yield higher current densities in MESs, but as obligate anaerobes, stringent culture conditions are required. In contrast, *Shewanella* sp. are facultative anaerobes, so exposure to oxygen is not detrimental and, as such, are easier to handle. *Shewanella* are also capable of transferring electrons to an unmatched array of terminal acceptors, making them an attractive choice for mechanistic studies in respiration, including EET. One of the most studied strains, *Shewanella oneidensis* MR-1 (MR-1) is both a model organism for EET mechanistic studies and a candidate organism for use within some of the proposed MES applications.[5]

Three distinct mechanisms have been proposed for MR-1 EET in MESs (Figure 1): 1) direct electron transfer (DET) between outer membrane cytochromes (MtrC/OmcA) and electrodes;[6] 2) long-ranged DET through conductive "wires"

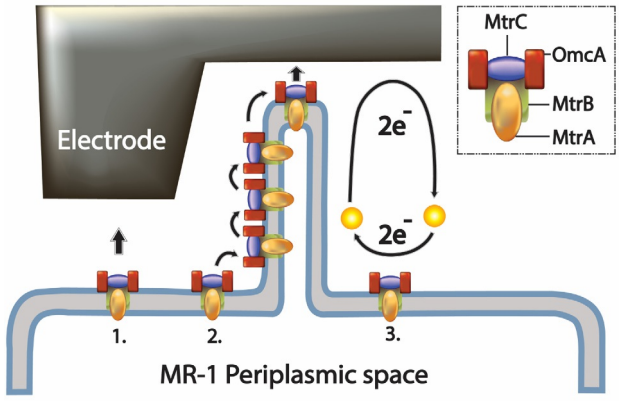

Figure 1. Overview of the three proposed mechanisms for MR-1 ET to electrodes. Electrons are passed onto the outer membrane spanning the MtrCAB/OmcA complex. From the MtrCAB/OmcA complex, ET to electrodes can occur directly with or without bound flavins as cofactors (1), through long-ranged DET involving wires formed by extrusions of the outer membrane and periplasm (2), or MET by flavins (3).

[a] *J. Oram, Dr. L. J. C. Jeuken*
School of Biomedical Sciences
and the Astbury Centre for Structural Molecular Biology
University of Leeds, Leeds LS2 9JT (UK)
E-mail: L.J.C.Jeuken@leeds.ac.uk

Supporting Information and the ORCID identification number(s) for the author(s) of this article can be found under http://dx.doi.org/10.1002/celc.201500505.

formed by extrusions of the outer membrane and periplasm,[7] in which electrons are thought to "hop" between the cytochromes that decorate these membrane extrusions;[8] 3) mediated electron transfer (MET) achieved through self-secreted redox mediators, in particular riboflavin (RF) and flavin mononucleotide (FMN), which shuttle electrons between the outer membrane cytochromes and electrodes.[9] FMN and RF have also been proposed to act as co-factors for MtrC and OmcA, respectively, in a DET mechanism.[10]

Whole-cell (in vivo) electrochemical studies of MR-1 have been performed on a variety of electrodes, ranging from gold and indium tin oxide (ITO) to carbon-based electrodes,[4,11,12] and a range of potentials have been reported for MET via flavins (between −0.25 and −0.13 V)[4,9] and DET via MtrC/OmcA (between 0 and +0.4 V).[4,6,12,13] The potentials reported for the DET mechanism are unexpected, as they are significantly higher than the decahemes MtrC and OmcA (between −0.4 to 0 V), which are thought to be the last step in the DET pathway.[14] This increased potential measured in vivo has been attributed to differences in the micro-environment at the microbe/electrode interface.[4]

The relevance of the different EET pathways in MES is under debate, with strong arguments for both MET and DET as the dominant pathway.[4,11,15] There is also significant variation in the reported redox potentials assigned to DET through MtrC/OmcA, as summarised in Table 1. This variation might be attributed to the different electrode materials used, but little is known about their surface properties and influence on MR-1s interaction with them. Recently, Artyushkova et al.[16] modified gold electrodes with different self-assembled monolayers (SAMs) and found that changing the electrode surface properties leads to significant differences in the morphology and current output of the bacterial biofilm. The EET mechanism to the different modified surfaces was not investigated by Artyushkova et al. Here, we adapted the approach of Artyushkova et al. to investigate the effect of surface properties on MR-1 EET mechanisms. Ultra-smooth gold electrodes were modified with SAMs terminated with different functional groups to alter the electrode surface charge. MR-1 was then grown on the SAM-modified gold electrodes along with pyrolytic carbon and ITO electrodes, and the EET mechanisms were studied with voltammetry.

2. Results

Rough, predominantly carbon-based electrodes are generally desired for MESs, as they exhibit large electrochemical surface areas for microbes to interface with, enabling higher currents and thus performance. In contrast, here we have employed ultra-smooth gold electrodes to enable the assembly of well-formed, uniform SAMs with reproducible surface characteristics that result in low capacitances, enabling sensitive voltammetric studies of the EET mechanism. Furthermore, to prevent complications in the analysis, owing to trace elements and other redox-active small molecules, a minimal electrolyte of 20 mM MOPS, 30 mM Na_2SO_4 and 10 mM sodium lactate was used in the majority of experiments.

MR-1 was first grown overnight, anaerobically in lysogeny broth (LB) supplemented with lactate and fumarate. The bacteria from the overnight culture were subsequently washed to remove growth medium and added to the electrochemical cells fitted with gold electrodes modified with SAMs of either pure 8-mecaptooctanol or a mixture of 8-mercaptooctanol and 8-mercapto-octanic acid. Both electrodes have hydrophilic surfaces, but the surface of the latter also has a negative surface charge. From here on, these electrodes will be designated as neutral and negative electrodes, respectively.

To encourage respiration with the electrodes, lactate was used as the sole carbon/electron source and the electrodes were poised at +0.25 V. After approximately 3 h, catalytic waves were observable with onsets that differed significantly between the two electrode surface types (at −0.2 and +0.1 V for the neutral and negative electrodes, respectively; Figure 2), confirming that the surface chemistry has a profound effect on the mechanism by which MR-1 transfers electrons to electrodes. When pyrolytic carbon electrodes were used, catalytic currents were much lower, but two oxidative signals were observed with onsets at −0.2 and +0.1 V (Figure S5), suggesting each onset is caused by a different EET mechanism and that the pyrolytic carbon electrodes can support both. Catalytic currents observed at an onset of about −0.2 V are commonly accepted to originate from an EET mechanism via flavins, either as freely diffusing electron mediators or bound as co-factors to outer membrane cytochromes.[4,9–11] As expected, when either

Table 1. A sample of the different experimental conditions used in MR-1 EET studies and the corresponding potentials ascribed to MR-1 DET.

Working electrode (WE)	WE potential during biofilm attachment [V vs. SHE]	Growth conditions in EC cell	Potential assigned to DET through MtrC/OmcA [V vs. SHE]	Ref.
5X-AQ carbon	+0.24	*Shewanella* basal medium (salts, minerals, vitamins and 15 mM lactate) buffered with 100 mM HEPES	ca. 0 (centred around)	[12]
carbon felt	−0.1	50 mM PBS, 100 mM lactate, 30 mM fumarate (for initial adaptation to respire on electrode)	+0.2 (onset of oxidation)	[11]
ITO	+0.4	DM containing 10 mM lactate, de-aerated with N_2, 30 °C	+0.05 (midpoint potential)	[6]
carbon rod	+0.4	minimal media (MM) including 18 mM lactate	+0.13±0.017 (formal potential)	[4]
glassy carbon	+0.24	LB prepared in 50 mM sodium phosphate buffer (pH 7.2)	ca. 0 (onset of oxidation)	[25]

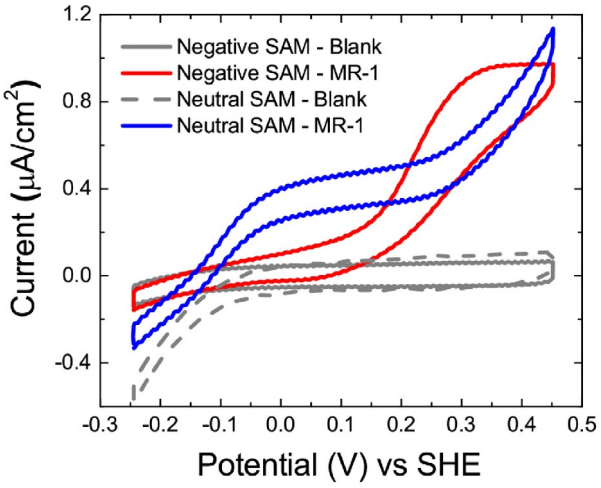

Figure 2. Cyclic voltammograms (CVs) of MR-1 grown on TSG modified with SAMs of either pure 8-OH (neutral surface, ——) or mixed 8-OH:8-COOH (negative surface, ——), after incubation with MR-1 ($OD_{600\,nm} \approx 0.3$) in 10 mM lactate, 20 mM MOPS, 30 mM Na_2SO_4, pH 7.4 at +0.25 V for approximately 22 h. Baselines measured before incubation with MR-1 for TSG electrodes modified with SAMs of 8-OH:8-COOH (——) and 8-OH (- - - -). All scans start at the immersion potential $E = 0$ V. Scan rate = 0.01 V s^{-1}.

RF or FMN was added, the catalytic wave retained the same onset potential, but the current increased.

To determine why different onset potentials were observed with neutral and negative electrodes, the electrochemical behaviour of flavin was determined with both electrodes. The reaction of riboflavin on neutral electrodes is reversible, indicating rapid ET, (Figure 3), whereas the electron exchange between riboflavin and negative electrodes (Figure 3) is indicative of a quasi- or irreversible ET reaction. The absence of an efficient ET reaction between flavin and negatively charged surface electrodes limits a flavin-mediated EET pathway and likely gives rise to the observed prevalence of an alternative EET pathway at higher potentials.

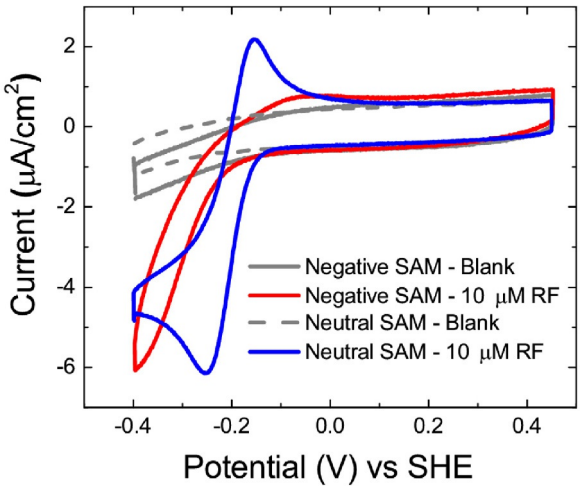

Figure 3. CVs of 10 μM RF, 20 mM MOPS, 30 mM Na_2SO_4 (pH 7.4) on TSG electrodes modified with SAMs of either pure 8-OH (neutral surface, ——) or mixed 8-OH:8-COOH (negative surface, ——). Baselines measured before incubation with RF for TSG electrodes modified with SAMs of 8-OH:8-COOH (——) and 8-OH (- - - -). All scans start at the immersion potential $E = 0$ V. Scan rate = 0.1 V s^{-1}.

Similar, higher potential onsets have previously been reported in the literature on carbon and ITO electrodes, and the EET pathway is proposed to be DET through MtrC/OmcA.[4,12,13] However, as discussed in the Introduction, the redox potentials of MtrC and OmcA do not overlap with the onset potential of the "high-potential" EET pathway. Therefore, further investigation into this alternative EET pathway was carried out. First, we tested whether the higher potential redox wave could be attributed to a redox compound released by MR-1 into the electrolyte. After growth on a negative electrode for about 23 h, the contents of the electrochemical cell were extracted and the electrolyte was separated from the bacteria by using centrifugation and 0.22 μm filtration. The filtered electrolyte was then analysed by using a fresh electrode (Figure 4). Importantly, the cyclic voltammogram shows redox signals at the same potential as the high-potential EET pathway, suggesting that this EET pathway involves a mediator.

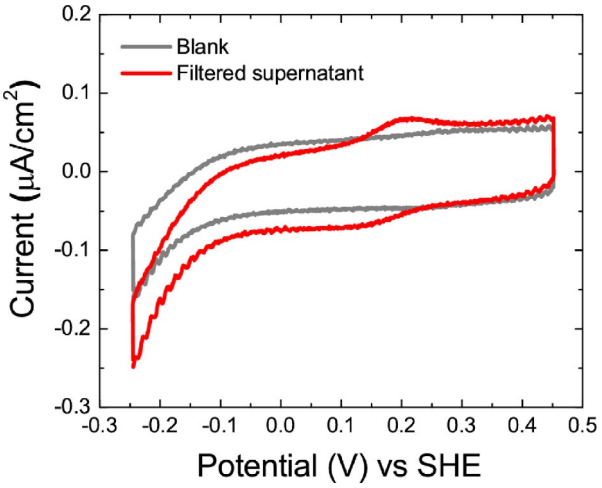

Figure 4. CVs of the growth medium used to grow MR-1 for approximately 23 h in a MES setup after removing MR-1 through centrifugation and filtration (0.22 μm), using a TSG electrode modified with a mixed SAM of 8-OH:8-COOH (negative surface, ——). Baselines measured before incubation with the growth medium (——). All scans start at the immersion potential $E = 0$ V. Scan rate = 0.01 V s^{-1}.

In an effort to identify the redox-active compound, the filtrate was analysed with LC-MS without success. To test if the redox-active compound was a cytochrome, the electrolyte was filtered through a 3 kDa cut-off filter. However, the redox-active compound passed through the filter, suggesting a molecular weight below 3 kDa. By elimination, we speculated the redox-active compound was an inorganic compound, most likely iron. Cyclic voltammograms of iron at negative electrodes (Figure 5) show a reversible ET reaction at the same onset potential as the high-potential EET pathway; whereas, with neutral surface electrodes (Figure S1), almost no redox signal is obtained. Importantly, lactate causes a large change in the Fe reduction signal, leading to a more reversible CV (Figure 5). It

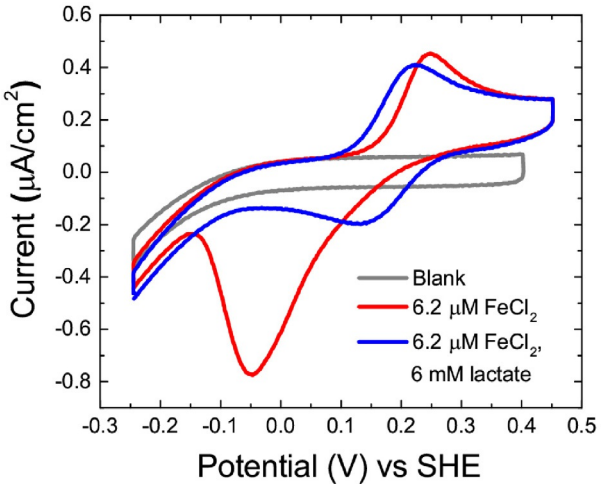

Figure 5. CVs of 6.2 μM $FeCl_2$ in 20 mM MOPS, 30 mM Na_2SO_4 (pH 7.4) on a TSG electrode modified with a mixed SAM of 8-OH:8-COOH (negative surface) before (——) and after addition of 6 mM lactate (——). Baselines measured before addition of $FeCl_2$ (——). All scans start at the immersion potential $E = 0$ V. Scan rate = 0.01 V s^{-1}.

should be noted that the reduction potential and voltammetry characteristics of Fe–lactate are remarkably similar to the non-turnover in vivo signals described in the literature as DET through MtrC/OmcA.[6,12]

To further confirm whether the high-potential EET pathway observed on negative electrodes originates from iron-based MET, deferoxamine was added. Deferoxamine is a siderophore that strongly chelates free iron, but is unable to dissociate iron from cytochromes such as MtrC and OmcA. Indeed, the addition of deferoxamine almost obliterates the high-potential EET pathway, leaving the smaller catalytic wave caused by flavin MET unaffected (Figure 6). A control CV of the Fe–deferoxamine complex confirms that this complex does not give reversible voltammetry signals on negatively charged electrodes (Figure S2). It is important to note that deferoxamine only complexes Fe^{III}, but under aerobic or micro-aerobic conditions facilitates "auto-oxidation" of Fe^{II} to Fe^{III}, as it influences the Fe^{II}/Fe^{III} redox equilibrium.[17] The results reported here were recorded under micro-aerobic conditions. Under strict anaerobic conditions ($O_2 < 0.1$ ppm using a glove box), it was observed that deferoxamine did not significantly affect the high-potential EET pathway, which we attribute to the reducing conditions, decreasing the ability of deferoxamine to complex iron. Importantly, under these strict anaerobic conditions, addition of 90 μM EDTA was still able to obliterate the high-potential EET pathway.

To rule out the possibility that deferoxamine is toxic to MR-1, an experiment was performed in which deferoxamine was added to MR-1 grown on a neutral SAM with exogenous RF (Figure S3). No effect was observed upon deferoxamine addition, nor was an effect observed upon prolonged incubation (> 30 min), confirming that deferoxamine, at the concentrations used here, has no detrimental effect on MR-1.

SAM-modified gold electrodes are not typically used in MESs, nor are supplemented MOPS buffers used as growth medium. For this reason, the experiments were repeated with more typical electrode materials, pyrolytic carbon and ITO, along with defined media (DM) as the growth medium. During incubation with MR-1, cyclic voltammetry was performed to examine the bacterial EET. On ITO electrodes, a high-potential signal is observed with an apparent midpoint potential of approximately +50 mV alongside a catalytic wave corresponding to flavin MET. This high-potential signal was, again, confirmed to originate from soluble iron upon the addition of deferoxamine (Figure 7). For a better comparison between ITO and SAM-modified gold electrodes, experiments were also performed with MOPS buffer supplemented with lactate and

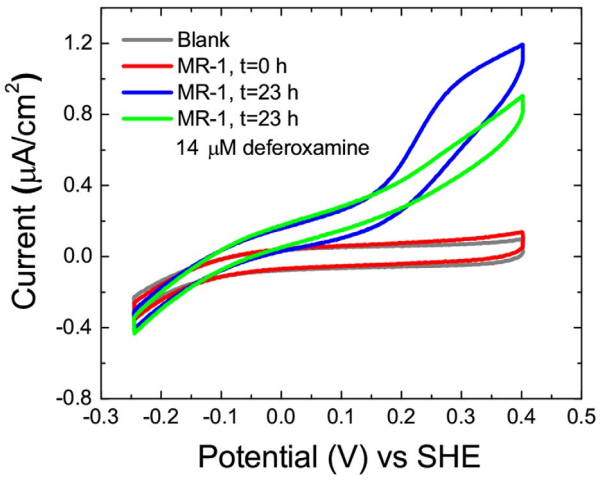

Figure 6. CVs of MR-1 ($OD_{600\,nm} = 0.55$) in 10 mM lactate, 20 mM MOPS, 30 mM Na_2SO_4 (pH 7.4), measured directly after addition of MR-1 (——), after 23 h incubation at +0.25 V (SHE, ——) and after addition of 14 μM deferoxamine and a further 30 min at 0.25 V (——), using a TSG electrode modified with a mixed SAM of 8-OH:8-COOH (negative surface). Baselines measured before addition of MR-1 (——). All scans start at the immersion potential $E = 0$ V. Scan rate = 0.01 V s^{-1}.

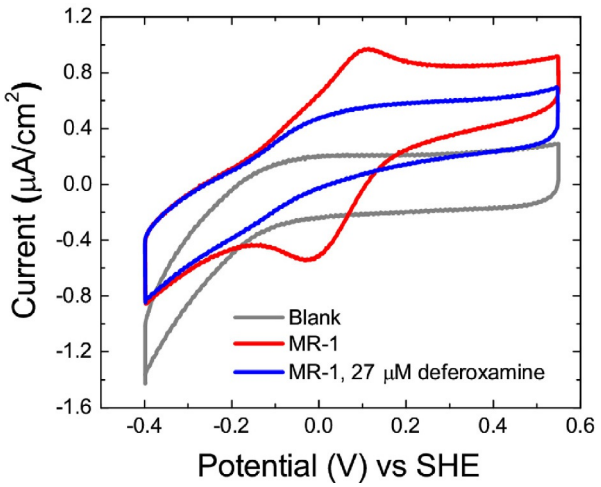

Figure 7. CVs with an ITO electrode after incubation with MR-1 at +0.4 V (SHE) for 21 h in DM medium before (——) and after (——) addition of 27 μM deferoxamine and a further 30 min incubation at +0.4 V (vs. SHE). Baselines measured before addition of MR-1 (——). All scans start at the immersion potential $E = 0$ V. Scan rate = 0.01 V s^{-1}.

a holding potential of +0.25 V (Figure S4). Under these conditions, the apparent midpoint potential of soluble iron on ITO was approximately +130 mV. Interestingly, the redox potential of high-potential peaks/signals on ITO (Figure 7) is shifted in the negative direction with respect to the negative gold (Figures 6 and S2) and pyrolytic carbon electrodes (Figure S5). Redox potentials of soluble iron are expected to depend on the electrolyte composition, as many anions have the propensity to coordinate to iron. Many media contain lactate, which will coordinate to iron, but additional factors such as pH will strongly influence the reduction potential. Furthermore, the surface properties of the electrode material will influence the interfacial ET kinetics, which can alter the onset of a catalytic wave.

3. Discussion

Artyushkova et al. previously performed a detailed study, in which the influence of the surface chemistry of SAM-modified gold electrodes on biofilm formation with MR-1 was investigated by using electrochemistry, confocal and electron microscopy.[16] Positively charged (amine-terminated SAMs) and hydrophilic (hydroxy-terminated SAMs) surfaces were found to present the most uniform biofilms. Importantly, as observed here, negatively charged surfaces (carboxylic-acid-terminated SAMs) were also found to support biofilm formation, although the films were more heterogeneous. In contrast to the work of Artyushkova et al., who used SAMs of pure mercaptoundecanoic acid to create negatively charged surfaces, here a mixture of 8-mercapto-1-octanol and 8-mercaptooctanoic acid (57:43 ratio) was used.

EET of MR-1 on hydroxy-terminated SAMs (neutral surface electrodes) is dominated by MET with a reversible ET reaction between the electrode and flavin. In contrast, on carboxylic-acid-terminated SAMs (negatively charged surface electrodes), ET from flavin to the electrodes becomes "sluggish" with a quasi-irreversible ET behaviour. On these electrodes, a second, alternative EET pathway becomes apparent at higher potential. Here, we have shown that this high-potential pathway is mediated by iron in solution. It is well known that MR-1 can use iron as a terminal electron acceptor,[18] and that iron (e.g. ferricyanide) can mediate ET from bacteria to the electrode.[19] Importantly, however, catalytic waves and redox signals similar to those reported here have previously been ascribed to DET through MtrC/OmcA,[4,12,13] but this assignment needs to be re-evaluated in light of the data presented here.

One principle reason for assigning the redox signals between 0 and 0.2 V to outer membrane cytochromes originates from NO-ligation experiments.[6] When NO was introduced to a biofilm of MR-1 grown on an ITO electrode, the signal at +50 mV disappeared and a new signal at +650 mV was observed. It was inferred that NO ligates with the hemes of outer membrane cytochromes, causing a shift in their redox potential. However, this same result would also be consistent with the fact that NO will ligate "free" iron in solution, raising the redox potential of the iron complexes.

The question of "what is the source of the extracellular iron" remains. The medium in the electrochemical experiments contained only buffer and lactate and can, therefore, be excluded as a source. It is also unlikely that significant concentrations of soluble iron were transferred when adding MR-1 to the electrochemical cells, as the MR-1 was washed twice in buffer prior to transfer. Furthermore, if iron was transferred with MR-1, it would have been immediately observable in the CV. Typically, the catalytic wave or non-turnover redox signals were not observed until more than 1 h incubation with MR-1. We, therefore, propose that iron is released from MR-1, either via active release (as is thought to be the case for flavins) or as a result of cell lysis. We propose that it is unlikely that MR-1 actively releases soluble iron, as iron is an essential trace nutrient for MR-1. The most likely cause of soluble iron accumulation is, therefore, cell lysis, where iron could be released from, for instance, iron storage proteins[20] into the electrolyte.

Although we cannot exclude DET as an EET pathway for MR-1, we propose that the "alternative" high-potential signals are caused by iron-mediated ET between MR-1 and the electrode. We, thus, recommend that iron chelators, such as deferoxamine, should be used to confirm or disprove DET mechanisms in future characterisations of MESs.

The absence of clearly distinguishable redox signals that can be ascribed to DET might question the extensive use of MR-1 as a model organism for EET in MESs. However, it has been shown that MR-1 is capable of significant DET to certain surfaces in its natural habitat, such as haematite.[21] Recently, there has been substantial effort directed towards novel electrode materials[22] and surface modifications of established electrode materials.[23] New materials could result in more suitable surfaces for DET with MR-1. DET is generally more desirable than MET in MESs, even if the microbe produces its own redox mediators like flavins, as the electrolyte in a MES is frequently or continuously replaced in certain applications. This would lead to the constant loss of mediator, impairing the electrochemical interaction between the electrode and microbes.

4. Conclusions

We have demonstrated that the surface properties of electrodes significantly impact EET pathways of MR-1 in MESs. Hydrophilic, non-charged electrodes (gold modified with hydroxy terminated SAMs) show favourable electron-transfer kinetics with flavin, enabling efficient ET between MR-1 and the electrode, with flavin as a mediator. However, negatively charged electrodes (gold modified with carboxylic-acid-terminated SAMs) exhibit quasi- or irreversible electron transfer with flavins, emphasising an alternative pathway, observable at higher potentials of approximately 0.1 V versus SHE. This high-potential pathway has previously been ascribed to MtrC/OmcA DET, but, through the addition of deferoxamine, we concluded that the alternative high-potential pathway in our system is mediated by soluble iron, possibly released by lysing MR-1. Similar iron-mediated EET could operate in other MESs, and this would explain the wide variation in redox potentials reported in the literature between groups using different electrodes and elec-

trolyte solutions. The redox potential of iron is dependent on its interactions with ligands in solution, for example lactate, as well as the surface properties of the electrode material. We urge future investigations to use mild iron chelators such as deferoxamine to confirm DET mechanisms. Finally, for MR-1 to be used in MES applications with high efficiency and performance, an anode material will need to be developed that promotes DET.

Experimental Section

Cultures and Media

All chemicals and materials were obtained from Sigma–Aldrich unless otherwise stated. *S. oneidensis* MR-1 cultures were grown aerobically in LB (30 °C, 200 rpm, 16 h) to an optical density $OD_{600\,nm} > 1$. This culture (1 mL) was used to inoculate LB (50 mL) supplemented with 50 mM lactate and 25 mM fumarate in a 50 mL falcon tube. The top of the tube was fastened shut and the culture was grown overnight (0 rpm, 30 °C). The bacteria reached a maximum $OD_{600\,nm}$ of approximately 0.7 and pH of 6.25–6.30 before growth ceased. The cells were pelleted by centrifugation (3220 g, 15 min) and washed twice with MOPS buffer (10 mL; 20 mM MOPS, 30 mM Na_2SO_4, pH 7.4) before re-suspension in MOPS buffer (5 mL). The washed MR-1 was stored at 4 °C and used as soon as possible (within 1–2 h) for electrochemical experiments.

DM contained the following ingredients (per litre): 1.5 g NH_4Cl (Melford), 0.1 g KCl (BDH laboratory supplies), 0.625 g Na_2HPO_4 (Melford), 0.213 g Na_2SO_4, 0.103 g $CaCl_2{\cdot}2H_2O$ (Fisher Scientific), 0.095 g $MgCl_2$ (ACROS organics), 1.51 g PIPES, 2 mL trace minerals solution and 10 mL vitamin solution. In addition to this, lactate was added to a concentration of 10 mM. The pH of DM was approximately 7.4, and it was sterilised by filter sterilisation (0.22 μm).

The trace minerals solution contained (per liter): 1 g $FeCl_2{\cdot}4H_2O$, 0.5 g $MnCl_2{\cdot}4H_2O$, 0.3 g $CoCl_2{\cdot}6H_2O$, 0.2 g $ZnCl_2$, 0.05 g $Na_2MoO_4{\cdot}2H_2O$ (ACROS organics), 0.02 g H_3BO_3, 0.1 g $NiSO_4{\cdot}6H_2O$, 0.002 g $CuCl_2{\cdot}2H_2O$ (ACROS organics), 0.006 g $Na_2SeO_3{\cdot}5H_2O$ and 0.008 g $Na_2WO_4{\cdot}2H_2O$ (ACROS organics). The vitamin solution contained (per liter): 0.002 g biotin, 0.002 g folic acid, 0.001 g B6 (pyridoxine) HCl, 0.005 g B1 (thiamine) HCl, 0.005 g B2 (riboflavin), 0.005 g nicotinic acid, 0.005 g pantothenic acid (Santa Cruz Biotechnology), 0.005 g *p*-aminobenzoic acid, 0.005 g lipoic acid, 0.2 g choline chloride and 0.001 g B12 (cobalamin) crystalline.

SAM-Modified Electrodes

Template-stripped gold (TSG) electrodes were prepared as described previously.[24] To form the SAMs, TSG glass slides were incubated in H_2O (1 mL) with 1 mM thiol, that is, either 8-mercapto-1-octanol (8-OH) or a 57:43 mixture of 8-OH and 8-mercaptooctanoic acid (8-COOH). Slides were incubated in the thiol solution at 4 °C for at least 16 h. Prior to use, the electrodes were washed with isopropanol and dried under a stream of N_2.

Electrochemistry

In general, for electrochemical experiments, a bespoke, glass, single-chamber electrochemical cell housed in a faraday cage was used with a standard three-electrode setup. As the working electrode, TSG (modified with a SAM) or ITO was embedded in a polytetrafluoroethylene (PTFE) holder with a rubber O-ring seal (exposing an electrode area of 0.24 cm^2). The working electrode was placed in the electrochemical cell along with a platinum-wire counter electrode and a saturated mercury/mercury sulfate (Hg/Hg_2SO_4) reference electrode (Radiometer analytical, France). All potentials were converted with respect to a standard hydrogen electrode (SHE), using +651 mV versus SHE for the Hg/Hg_2SO_4 reference electrode. MOPS buffer, continuously purged with argon, was used as the basal electrolyte solution for all experiments, unless stated otherwise. For a typical experiment, washed MR-1 was added to the electrochemical cell to $OD_{600\,nm} = 0.45$. Sodium lactate was then added from a 200 mM stock solution to a final concentration of 10 mM (acting as the sole electron/carbon source for bacterial respiration). To promote EET to the working electrode, the electrode was poised at +0.25 V (vs. SHE). At various time points, the interaction of bacteria on the SAM-modified electrodes was probed with cyclic voltammetry. Small variations to this general method are detailed, where relevant, in the Results section. In some experiments, a DM was used instead of MOPS buffer as the basal electrolyte solution.

Electrochemical experiments with pyrolytic graphite edge (PGE) electrodes followed the same experimental method as described for TSG electrodes, but required a different experimental setup. A bespoke, two-chamber, glass electrochemical cell housed in a faraday cage was used with a standard three-electrode setup. The PGE working electrode (geometrical area ca. 0.24 cm^2) was inserted, along with a platinum-wire counter electrode, into the main chamber and a saturated mercury/mercury sulfate (Hg/Hg_2SO_4) reference electrode was inserted into the side chamber. The two chambers were interconnected with a narrow glass tube, allowing for the diffusion of electrolytes between the two chambers.

Electrochemical measurements were obtained by using an Autolab electrochemical analyser (Ecochemie, Utrecht, Netherlands) equipped with a PGSTAT 128N potentiostat, SCANGEN and ADC750 modules, and FRA2 frequency analyser (Ecochemie). Cyclic voltammetry measurements were routinely carried out by holding the potential at 0 V for 5 s before cycling between +0.4 and −0.4 V (vs. SHE) at a scan rate of 10 or 100 $mV\,s^{-1}$. All electrochemical experiments reported here were performed at 20 °C.

Supernatant Analysis

MR-1 with $OD_{600\,nm} = 0.25$ was incubated for approximately 22 h in MOPS buffer (2 mL) with 10 mM sodium lactate on a 8-OH:8-COOH (57:43) mixed SAM-modified TSG electrode, which was poised at +0.25 V (vs. SHE). To separate the cells from the supernatant, the contents of the EC cell were centrifuged at 4500 *g* and filtered through a 0.22 μm polyethersulfone (PES) filter. The filtered supernatant was analysed by using voltammetry with fresh TSG electrodes that were prepared as described above.

Acknowledgements

The research leading to these results has received funding from the European Research Council under the European Union's Seventh Framework Programme (FP/2007-2013)/ERC Grant no. 280518.

Keywords: deferoxamine · electrochemistry · electron transfer · iron · microbial systems

[1] B. E. Logan, K. Rabaey, *Science* **2012**, *337*, 686 – 690.
[2] S. F. D'Souza, *Biosens. Bioelectron.* **2001**, *16*, 337 – 353; F. Golitsch, C. Buecking, J. Gescher, *Biosens. Bioelectron.* **2013**, *47*, 285 – 291; H. H. Hau, J. A. Gralnick, *Annu. Rev. Microbiol.* **2007**, *61*, 237 – 258; K. Rabaey, W. Verstraete, *Trends Biotechnol.* **2005**, *23*, 291 – 298.
[3] T. A. Clarke, M. J. Edwards, A. J. Gates, A. Hall, G. F. White, J. Bradley, C. L. Reardon, L. Shi, A. S. Beliaev, M. J. Marshall, Z. Wang, N. J. Watmough, J. K. Fredrickson, J. M. Zachara, J. N. Butt, D. J. Richardson, *Proc. Natl. Acad. Sci. USA* **2011**, *108*, 9384 – 9389; M. A. Firer-Sherwood, K. D. Bewley, J.-Y. Mock, S. J. Elliott, *Metallomics* **2011**, *3*, 344 – 348.
[4] A. A. Carmona-Martinez, F. Harnisch, L. A. Fitzgerald, J. C. Biffinger, B. R. Ringeisen, U. Schroeder, *Bioelectrochemistry* **2011**, *81*, 74 – 80.
[5] R. S. Hartshorne, C. L. Reardon, D. Ross, J. Nuester, T. A. Clarke, A. J. Gates, P. C. Mills, J. K. Fredrickson, J. M. Zachara, L. Shi, A. S. Beliaev, M. J. Marshall, M. Tien, S. Brantley, J. N. Butt, D. J. Richardson, *Proc. Natl. Acad. Sci. USA* **2009**, *106*, 22169 – 22174; L. Shi, K. M. Rosso, T. A. Clarke, D. J. Richardson, J. M. Zachara, J. K. Fredrickson, *Front. Microbiol.* **2012**, *3*, 50.
[6] A. Okamoto, R. Nakamura, K. Hashimoto, *Electrochim. Acta* **2011**, *56*, 5526 – 5531.
[7] S. Pirbadian, S. E. Barchinger, K. M. Leung, H. S. Byun, Y. Jangir, R. A. Bouhenni, S. B. Reed, M. F. Romine, D. A. Saffarini, L. Shi, Y. A. Gorby, J. H. Golbeck, M. Y. El-Naggar, *Proc. Natl. Acad. Sci. USA* **2014**, *111*, 12883 – 12888.
[8] N. S. Malvankar, D. R. Lovley, *Curr. Opin. Biotechnol.* **2014**, *27*, 88 – 95.
[9] E. Marsili, D. B. Baron, I. D. Shikhare, D. Coursolle, J. A. Gralnick, D. R. Bond, *Proc. Natl. Acad. Sci. USA* **2008**, *105*, 3968 – 3973.
[10] A. Okamoto, K. Saito, K. Inoue, K. H. Nealson, K. Hashimoto, R. Nakamura, *Energy Environ. Sci.* **2014**, *7*, 1357 – 1361.
[11] J. N. Roy, S. Babanova, K. E. Garcia, J. Cornejo, L. K. Ista, P. Atanassov, *Electrochim. Acta* **2014**, *126*, 3 – 10.
[12] D. Baron, E. LaBelle, D. Coursolle, J. A. Gralnick, D. R. Bond, *J. Biol. Chem.* **2009**, *284*, 28865 – 28873.
[13] J. N. Roy, K. E. Garcia, H. R. Luckarift, A. Falase, J. Cornejo, S. Babanova, A. J. Schuler, G. R. Johnson, P. B. Atanassov, *J. Electrochem. Soc.* **2013**, *160*, H866 – H871.
[14] M. Breuer, K. M. Rosso, J. Blumberger, J. N. Butt, *J. R. Soc. Interface* **2015**, *12*, 20141117; M. Firer-Sherwood, G. S. Pulcu, S. J. Elliott, *J. Biol. Inorg. Chem.* **2008**, *13*, 849 – 854.
[15] N. J. Kotloski, J. A. Gralnick, *mBio* **2013**, *4*, e00553-12.
[16] K. Artyushkova, J. A. Cornejo, L. K. Ista, S. Babanova, C. Santoro, P. Atanassov, A. J. Schuler, *Biointerphases* **2015**, *10*, 019013.
[17] J. A. R. Worrall, Y. J. Liu, P. B. Crowley, J. M. Nocek, B. M. Hoffman, M. Ubbink, *Biochemistry* **2002**, *41*, 11721 – 11730.
[18] D. Coursolle, J. A. Gralnick, *Front. Microbiol.* **2012**, *3*, 56.
[19] R. Emde, A. Swain, B. Schink, *Appl. Microbiol. Biotechnol.* **1989**, *32*, 170 – 175.
[20] K. Chourey, W. Wei, X.-F. Wan, D. K. Thompson, *BMC Genomics* **2008**, *9*, 395.
[21] B. H. Lower, L. Shi, R. Yongsunthon, T. C. Droubay, D. E. McCready, S. K. Lower, *J. Bacteriol.* **2007**, *189*, 4944 – 4952; L. A. Meitl, C. M. Eggleston, P. J. S. Colberg, N. Khare, C. L. Reardon, L. Shi, *Geochim. Cosmochim. Acta* **2009**, *73*, 5292 – 5307.
[22] S. Singh, N. Verma, *Int. J. Hydrogen Energy* **2015**, *40*, 5928 – 5938; Z. Luo, D. Yang, G. Qi, L. Yuwen, Y. Zhang, L. Weng, L. Wang, W. Huang, *ACS Appl. Mater. Interfaces* **2015**, *7*, 8539 – 8544.
[23] J. Du, C. Catania, G. C. Bazan, *Chem. Mater.* **2014**, *26*, 686 – 697; J. A. Cornejo, C. Lopez, S. Babanova, C. Santoro, K. Artyushkoya, L. Ista, A. J. Schuler, P. Atanassov, *J. Electrochem. Soc.* **2015**, *162*, H597 – H603.
[24] D. Stamou, D. Gourdon, M. Liley, N. A. Burnham, A. Kulik, H. Vogel, C. Duschl, *Langmuir* **1997**, *13*, 2425 – 2428.
[25] L. Peng, S.-J. You, J.-Y. Wang, *Biosens. Bioelectron.* **2010**, *25*, 2530 – 2533.

Manuscript received: November 20, 2015
Accepted Article published: February 12, 2016
Final Article published: February 19, 2016

